Submitted to the International Conference on High Energy Physics, ICHEP 98,
Vancouver, Canada, July 1998

Measurement of the Di-jet Cross Section in Photoproduction at HERA

H1 Collaboration

Abstract

Using 1996 data collected by the H1-collaboration at the HERA-collider the differential di-jet cross section $d\sigma/dx_\gamma^{jets}$ is measured in photoproduction processes. The kinematic range covered extends down to small parton fractional energies of $x_\gamma = 0.04$, where the gluon content of the photon is largely unknown.

Abstract 549
Parallel Sessions 5,3
Plenary Sessions 7,5

1 Introduction

In perturbative QCD, hadronic scattering processes of a proton with a quasi-real photon can be described as a scattering of partons in the photon and proton. Previous measurements of deep inelastic $e\gamma$ processes at e^+e^- colliders (PETRA and LEP) led to a determination of the quark content in the photon. In comparison the di-jet cross section in photoproduction processes at HERA [1, 2, 3, 4, 5] is sensitive to the gluonic component of the photon especially at lower x_γ, where the gluon content of the photon is still not well known.

In this analysis di-jet events of the 1996 data of the H1 experiment at HERA are used to determine the di-jet cross section as function of x_γ. The integrated luminosity corresponds to 7.2 ± 0.14 pb^{-1}, which is an increase by a factor of 3.6 compared to previous analyses of H1 [1, 2, 3]. These analyses are extended here towards lower transverse energy of the jets in order to access the low x_γ region. A complementary analysis of the gluon content in the photon based on the measurement of single charged tracks is discussed in [6].

2 Event Selection and Kinematic Reconstruction

The H1 detector is described in detail elsewhere [7]. The main components used in this analysis are the electron tagger situated 33m downstream of the interaction region to detect electrons scattered at small angles, the central tracking chambers which cover the polar angle region $20^0 < \theta < 160^0$ and the liquid argon (LAr) calorimeter ($4^0 < \theta < 153^0$).

For the jet finding and the kinematic reconstruction both tracks reconstructed in the central tracking detector and clusters found in the calorimeters are used. To avoid double counting of energies, regions in the calorimeters associated to tracks are masked. Only tracks with low momentum ($P < 1.5$ GeV) are considered to avoid artificial jets based on single, badly measured tracks.

The following criteria are used for the data selection:

- The event must have been triggered by a combination of sub-triggers from the electron tagger and charged tracks in the central detectors.
- The scattered positron has to be measured in the tagger in order to ensure a low photon virtuality ($Q^2 < 0.01$ GeV^2). The energy fraction y_e carried by the radiated photon is restricted to the range $0.5 < y_e < 0.7$, where y_e is reconstructed from the tagged electron energy,
$$y_e = 1 - \frac{E_{e,tagged}}{E_{e,beam}}.$$
- At least two jets with transverse energy $E_{T,jet} > 4$ GeV and an invariant jet-jet mass $M_{12} > 12$ GeV have to be found by a cone algorithm [8, 9, 10] in the region $-0.5 < \eta_{jet} < 2.5$, where η_{jet} is the pseudorapidity in the laboratory and negative η correspond to the direction of the outgoing positron. A small cone radius of $R = 0.7$ in the $\eta - \phi$ plane is used in order to minimize the effects of the underlying event energy on the jet energy measurement.
- The difference in η between the jets has to be small, $|\eta_1 - \eta_2| < 1$.

The above cuts on the jet variables are chosen to ensure a hard scale for the scattering process, a good correlation between the reconstructed and generated jets in the simulation and a sufficient resolution for x_γ. The cut on y_e implies that a high momentum photon enters the hard scattering process such that the produced jets remain well within the acceptance of the detector.

The momentum fraction of the incident parton in the photon is reconstructed using y_e and the transverse energies and pseudorapidities of the two jets with the highest E_T,

$$x_\gamma^{jets} = \frac{E_{T,jet1}e^{-\eta_{jet1}} + E_{T,jet2}e^{-\eta_{jet2}}}{2\, y_e\, E_{e,beam}}.$$

The lower cut on the transverse energy and the invariant mass of the jets and the upper limit on the pseudorapidity and y_e restrict the measurement of the di-jet cross section to the range $x_\gamma > 0.03$.

The trigger efficiency is monitored in the data by using an independent reference trigger. The efficiency ranges from 90% at high x_γ to 65% at low x_γ, and is well described by the detector simulation. An error of $\pm 5\%$ is assigned to the trigger efficiency. The event rate is stable as function of the integrated luminosity. Using the above selection cuts 1889 di-jet events remain.

3 Cross Section Measurement

In the following the hadronic di-jet cross section is evaluated by correcting the measured event distributions for detector effects. These are determined by applying a detailed detector simulation to photoproduction events generated by two different Monte Carlo models, PHOJET1.06 [11] and PYTHIA5.7 [12]. Both models use leading order QCD matrix elements folded with parton density functions of the photon and proton to describe the hard scattering process. However they differ considerably in their conceptual description of the underlying event [11, 12].

The yield of di-jet events depends on the hard scattering process as well as on the underlying event. Both components are seen in figure 1, where the uncorrected jet profiles as function of azimuthal angle for two $E_{T,jet}$-regions are shown. Jets are clearly visible both at high and at low $E_{T,jet}$. The jet shapes as well as the amount of energy between jets due to the underlying event is well described by both Monte Carlo models.

In figure 2 the correlation between the reconstructed value of x_γ and the x_γ-value determined using jets on the hadron level is shown using the PHOJET model. The good correlation also at low x_γ is mainly due to the cut on the invariant mass of the two jets and allows to determine the corrected di-jet cross section in x_γ up to $x_\gamma > 0.04$ using an unfolding method [13].

The uncorrected data distributions for x_γ, for the distance in pseudorapidity between the two jets, the pseudorapidity of the highest E_T-jet, the invariant mass of the two jets and their mean E_T distribution are shown in figure 3 and 4. All distributions are well described by the PHOJET model (shown) as well as by the PYTHIA model (not shown) after applying correction factors obtained by the unfolding procedure.

In figure 5 the ep di-jet cross section is shown as function of x_γ. The cross section is corrected for all detector effects and is valid in the kinematic region $E_{T,jet1,2} > 4\, GeV$, $M_{jet1,2} > 12\, GeV$, $-0.5 < \eta_{jet1,2} < 2.5$, $|\eta_{jet1} - \eta_{jet2}| < 1$ and $0.5 < y_e < 0.7$. The inner error bars reflect the statistical error, the outer error bars show the statistical and systematical error added in quadrature. The dominant error (up to 24% at low x_γ) results from the uncertainty of the knowledge of the hadronic energy scale which is known to $\pm 4\%$. Using the LAC1- [14], GRV- [15] and a flat parton density function for the photon as start for the unfolding procedure leads to an uncertainty of the final cross section of less than 10%. The detector corrections are found to differ by up to 10% using the PHOJET and PYTHIA model for the unfolding with $1/2E_T$ and E_T for the renormalisation scale. Additional experimental uncertainties arise due to the luminosity measurement (2%), the trigger efficiency (5%) and the acceptance of the electron tagger (5%). All systematic errors are added in quadrature.

The measured cross section is compared to the prediction of the PHOJET model using the GRV-LO parton density functions for the photon and the proton. Here the transverse energy E_T is used for both the factorisation and renormalisation scale.

Also shown in figure 5 are the different contributions from direct photon induced processes as well as from resolved photon processes, where either quarks or gluons contribute. The cross section is well constrained by the measurement also at low $x_\gamma (x_\gamma > 0.04)$. In this region the quark contribution, which is obtained from LO calculations of PHOJET is significantly smaller than the measured cross section and allows for a large gluon component in the photon. It is noted that current parton density parametrisations of the photon [15, 14] differ in this region by large factors in their absolute gluon flux.

4 Conclusion

A new measurement of the differential di-jet cross section $d\sigma/dx_\gamma^{jets}$ in the photoproduction regime of HERA is presented, which extends the previously accessible range of the parton fractional energy x_γ^{jets} down to $x_\gamma^{jets} = 0.04$. The error in the measured cross section is considerably smaller than the uncertainty in the theoretical prediction of the di-jet cross section due to the lack of knowledge of the gluon content in the photon and the scale uncertainty of leading order QCD matrix elements.

Acknowledgements

We are grateful to the HERA machine group whose outstanding efforts have made and continue to make this experiment possible. We thank the engineers and technicians for their work in constructing and now maintaining the H1 detector, our funding agencies for financial support, the DESY technical staff for continual assistance, and the DESY directorate for the hospitality which they extend to the non-DESY members of the collaboration.

References

[1] H1 Collab, T. Ahmed *et al.*, *Nucl. Phys.* B **445**, 195 (1995).

[2] H1 Collab, S.Aid *et al.*, *Z. Phys.* C **70**, 17 (1996).

[3] H1 Collab, T. Ahmed*et al.*, *Eur.Phys.J.* C **1**, 97 (1998).

[4] ZEUS Collab, M. Derrick *et al.*, *Phys. Lett.* B **322**, 287 (1994).

[5] ZEUS Collab, M. Derrick *et al.*, *Phys. Lett.* B **384**, 401 (1996).

[6] H1 Collaboration: "Gluon Density in the Photon Extracted Using High pT Charged Particles in Photoproduction at HERA", paper 270 submitted to International Europhysics Conference on High Energy Physics, HEP97 August 9-26 1997 Jerusalem, Israel.

[7] H1 Collab., I. Abt *et al.*, *Nucl. Instrum. Methods* A **386**, 310-396 (1997).

[8] J. Huth *et al.*, Proceedings of the Summer Study on High Energy Physics, Snowmass, Colorado, 1990, 134

[9] CDF Collaboration, F. Abe *et al.*, *Phys. Rev.* D **45**, 1448 (1992)

[10] L.A. del Pozo, PhD Thesis University of Cambridge, RALT-002, 1993

[11] "PHOJET" Monte Carlo, R. Engel; R. Engel, *Z. Phys.* C **66**, 203 (1995).

[12] T. Sjöstrand, CERN-TH-6488 (1992), Comput. Phys. Commun. 82 (1994) 74.

[13] G. D'Agostini, *Nucl. Instrum. Methods* A **362**, 487 (1995).

[14] H. Abramowicz, K. Charchula, A. Levy, *Phys. Lett.* B **269**, 458 (1991).

[15] M. Glück, E. Reya, M. Stratmann, *Phys. Rev.* D **46**, 1973 (1992).

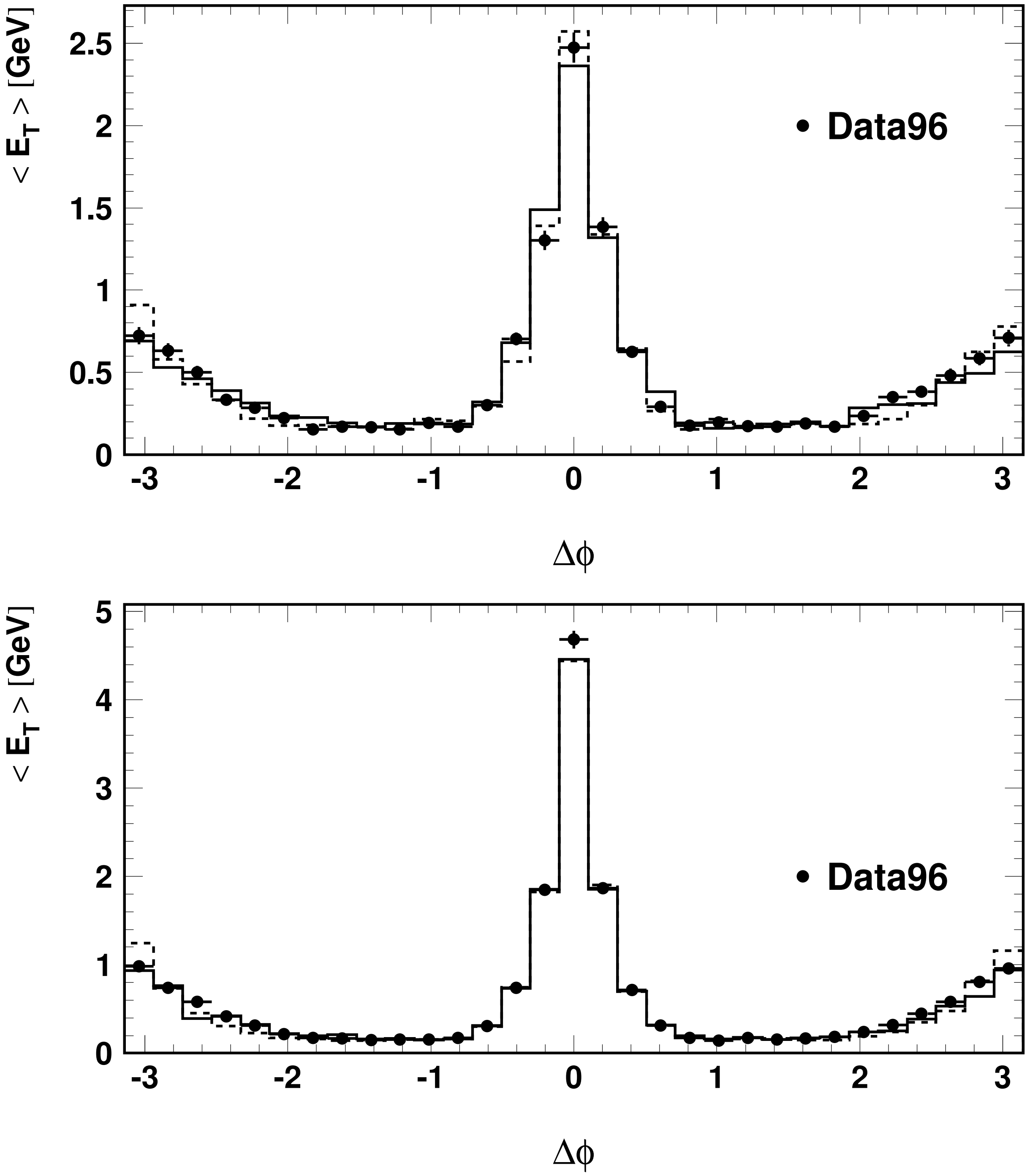

Figure 1: Observed transverse energy flow around the jet axis projected onto the azimuthal direction, for $E_{T,jet} < 7.5GeV$ (upper figure) and $E_{T,jet} > 7.5GeV$ (lower figure). The full (dashed) line shows the energy flow predicted by the PYTHIA (PHOJET) generator including detector effects.

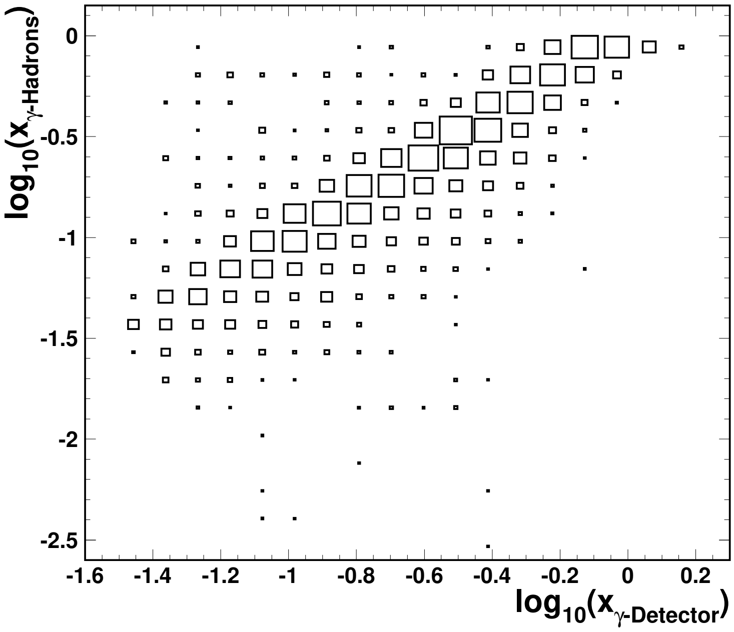

Figure 2: Correlation between x_γ calculated from jets found on the hadron level and the reconstructed x_γ from jets on detector level for the PHOJET model.

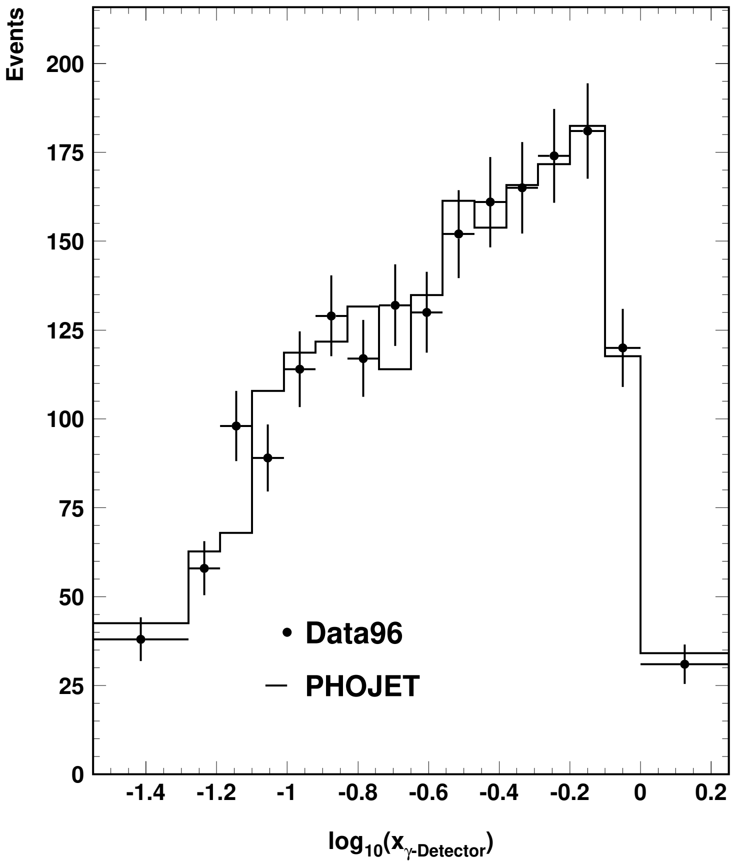

Figure 3: Uncorrected x_γ-distribution of di-jet events compared to the corrected PHOJET model prediction (full line, see text).

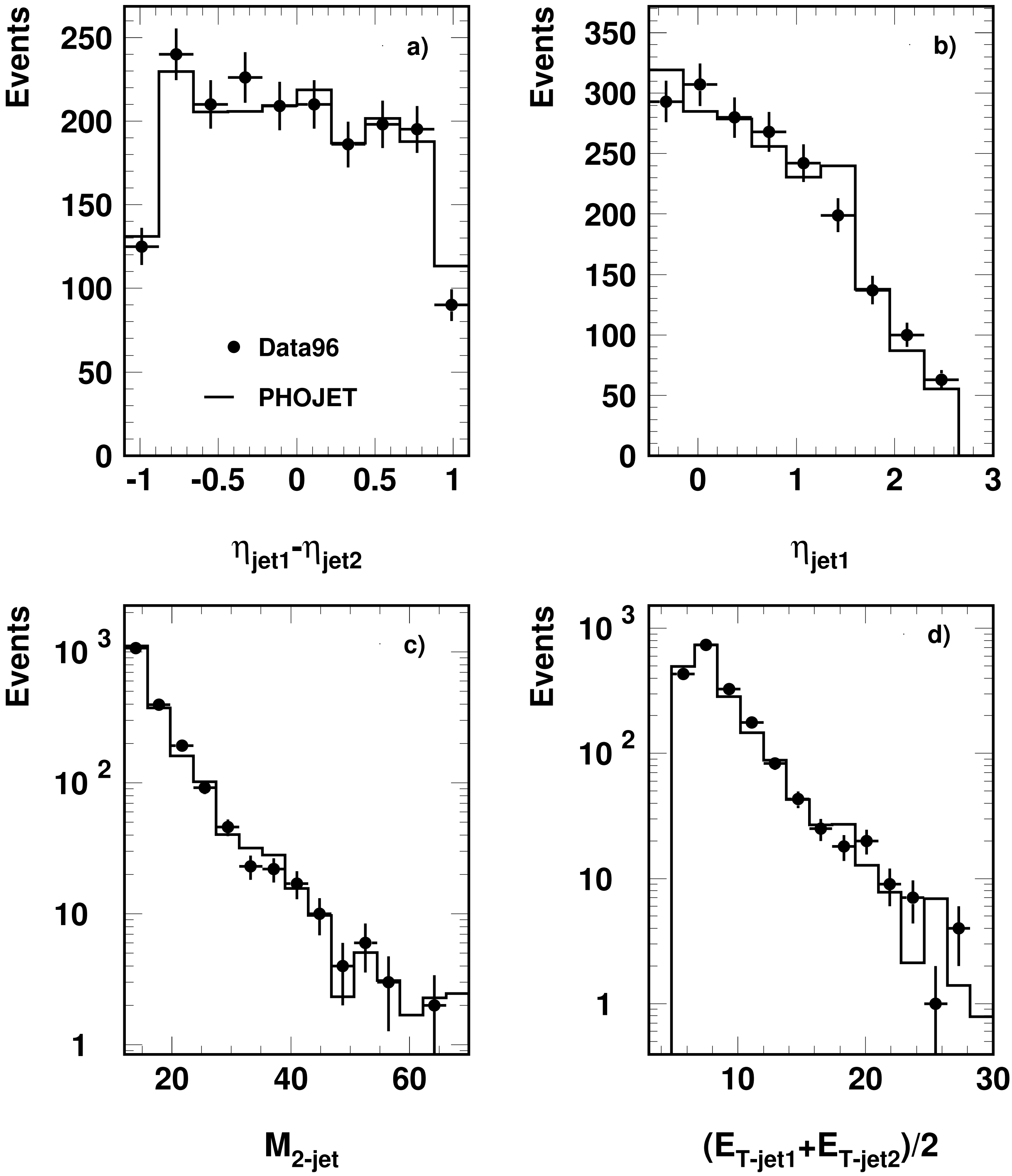

Figure 4: Kinematic distributions of jets for data (points) and the corrected Monte Carlo model PHOJET (full line). Figure a) shows the distance in pseudorapitidy between the two jets, b) the pseudorapitidy of the jet with the highest E_T, c) the invariant mass of the two jets and d) the mean E_T of the two jets.

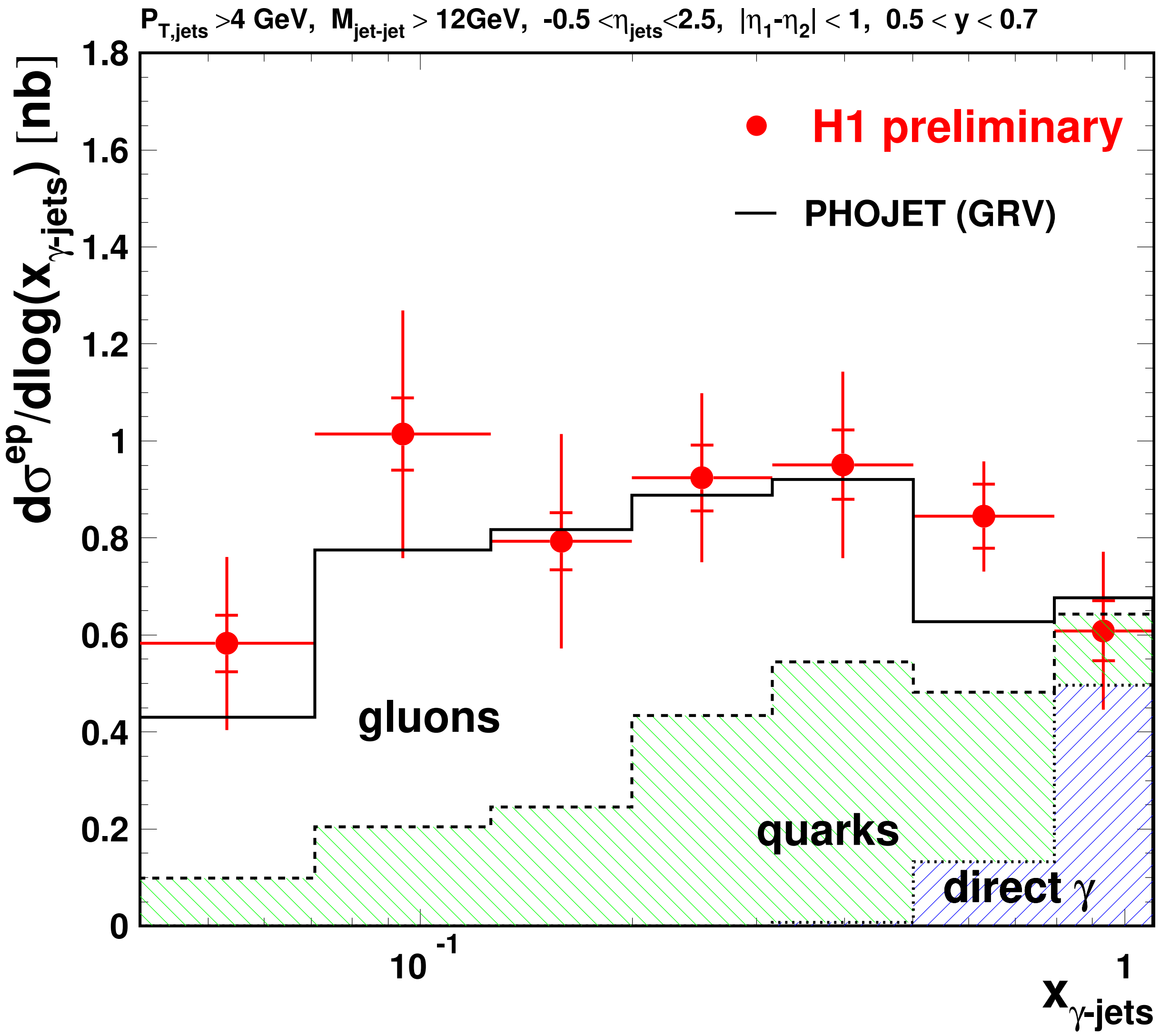

Figure 5: The measured di-jet cross section in photoproduction processes at HERA as function of x_γ. The jets were found with the CDFCONE-algorithm ($R = 0.7$). The data are compared to the LO QCD calculation of PHOJET with the GRV-LO parton density functions for the photon and proton and E_T for the factorisation and renormalisation scale. Also indicated are the different contributions of direct photon processes and resolved photon processes, where either quarks or gluons contribute.